

# Fabrication of Patterned Polystyrene Nanotube Arrays in an Anodic Aluminum Oxide Template by Photolithography and the Multiwetting Mechanism

Xiaoru Li,<sup>†</sup> Yiqian Wang,<sup>‡</sup> Guojun Song,<sup>\*,†</sup> Zhi Peng,<sup>†</sup> Peidong Li,<sup>†</sup> Qing Lin,<sup>‡</sup> Ning Zhang,<sup>§</sup> Zhifeng Wang,<sup>§</sup> and Xiaofeng Duan<sup>§</sup>

*Institute of Polymer Materials, Qingdao University, No. 308 Ningxia Road, Qingdao 266071, P.R. China, Laboratory of Advanced Fiber Materials and Modern Textile, the Growing Base for State Key Laboratory, Qingdao University, No. 308 Ningxia Road, Qingdao 266071, P.R. China, and Beijing Laboratory of Electron Microscopy, Beijing National Laboratory for Condensed Matter Physics, Institute of Physics, Chinese Academy of Sciences, Beijing 100080, P.R. China*

Received: May 7, 2009; Revised Manuscript Received: June 26, 2009

Patterned polystyrene (PS) nanotube arrays were successfully fabricated using photolithography via the polymer solution-wetting method. The microstructure of these nanotubes was investigated using conventional and high-resolution transmission electron microscopy (HRTEM). Two major types of morphology were observed for these PS nanotubes, one being bamboo-like and the other being barrel-shaped. The multiwetting mechanism was proposed to explain the different morphologies. X-ray diffraction (XRD) showed that the PS nanotubes have a higher degree of crystallinity than bulk PS. In addition, crystalline lattice fringes were observed in some regions of the PS nanotubes using HRTEM. Patterned polymer nanotube arrays could be used for nanocable coating to protect from oxidation and corrosion in nanodevices.

## 1. Introduction

Polymer tubular nanostructures have attracted a great deal of interest during the past decade because of their potential applications in nanoelectronic devices, ultrafiltration, catalysis, medicine, separation, and sensors.<sup>1–6</sup> Tubular nanostructures can be prepared by various synthesis methods.<sup>7–10</sup> The template synthesis method is regarded as a simple and very effective way for preparing various materials, including polymers, metals, semiconductors, carbon, and other materials.<sup>9,11–14</sup> Porous alumina template synthesis is one of the most commonly used methods because of the walls exhibiting a high surface energy. The polymer nanotubes can be obtained by wetting the porous templates with polymer melts or solutions. It is well-known that most bulk polymers are spherulites when they crystallize. Polymer nanotubes obtained from polymer melts or solutions can be crystalline. We investigated these phenomena for the particular case of polystyrene (PS) nanotubes.

With the development of nanotechnology, many groups have focused on obtaining patterns with the smallest possible lateral dimensions.<sup>15</sup> Micro- and nanometer-scale patterns can be obtained by photolithography,<sup>16</sup> electron-beam lithography,<sup>17</sup> soft lithography,<sup>18</sup> and microcontact printing ( $\mu$ CP).<sup>19,20</sup> These techniques have partially the same process: they can transfer patterns onto a substrate. Among these techniques, photolithography is one of the most successful techniques in large-scale microfabrication.<sup>20</sup> The method is convenient, effective, and simple. It could be used to deposit metal nanowire arrays with different patterns, and to fabricate polymer nanostructures with various patterns.<sup>10</sup>

Here, we describe a detailed fabrication procedure of patterned polymer nanotube arrays using photolithography via the polymer solution-wetting method in a porous alumina mem-

brane, and propose a solution-wetting mechanism for the PS nanotubes. Nanotube arrays will be used for nanocable coatings to protect metal nanowires from oxidation and corrosion in nanodevices. Crystallization of PS nanotubes was investigated by X-ray diffraction (XRD) and high-resolution transmission electron microscopy (HRTEM). The synthesis method and solution-wetting mechanism are all applicable to fabricate other polymer nanotube arrays.

## 2. Experimental Section

**2.1. Materials.** A porous anodic aluminum oxide (AAO) template (purchased from Whatman International Ltd.) was used with the pore diameter ranging from 180 to 300 nm and the depth ranging from 50 to 60  $\mu$ m. It was treated in alcohol in an ultrasonic bath to clean its surface before it was used. BP-212 (Beijing Kehua Fengyuan Microelectronic Technology Co., Ltd.) was used as a photoresist.

**2.2. Preparation of Patterned AAO Membrane.** The AAO template was spin-coated with a layer of photoresist at 2700 rpm for 30 s to seal the pores and then “soft baked” at low temperature (313 K) in order to remove the solvents from the photoresist and improve photoresist–AAO template adhesion. This composite was covered with a photolithographic mask and exposed to ultraviolet light (UV 365 nm) for 20 s. Subsequently, the sample was “hard baked” at higher temperature (363 K) to further activate cross-linking processes and to improve the mechanical stability of the pattern. Afterward, the sample was developed, flushed with deionized water several times, and dried in nitrogen. The pores of AAO were selectively opened only in the exposed areas.

**2.3. Solution Wetting of Polymer Nanotubes.** A drop of PS (2.5 wt %) solution was placed on a microscope slide, and then, an AAO membrane with the patterned side downward was quickly placed on it. The solution entered completely into the template open pores along their inner walls. Then, the composite was placed in a sodium hydroxide solution to dissolve the

\* Corresponding author. E-mail: songguojunqdu@126.com.

<sup>†</sup> Institute of Polymer Materials, Qingdao University.

<sup>‡</sup> The Growing Base for State Key Laboratory, Qingdao University.

<sup>§</sup> Chinese Academy of Sciences.

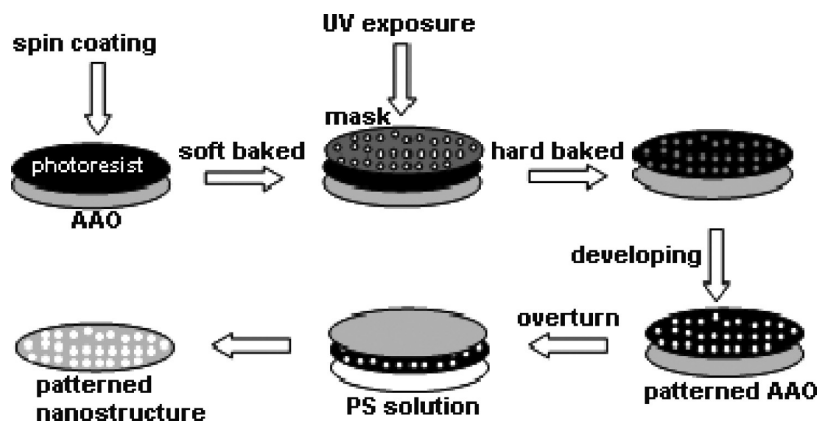


Figure 1. Schematic diagram for nanofabrication.

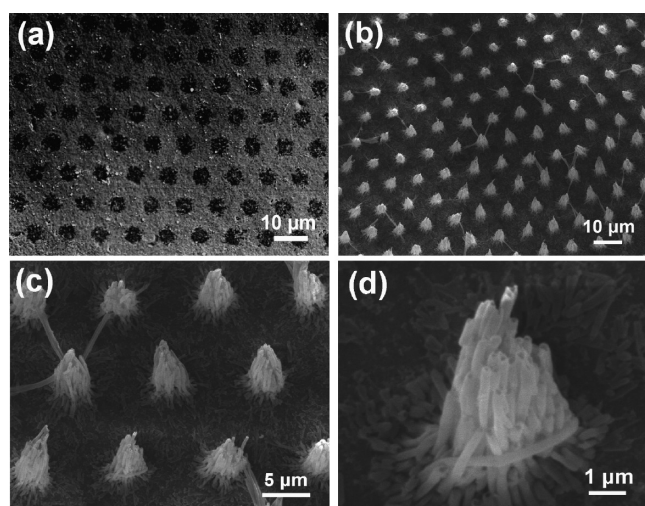


Figure 2. (a) Typical SEM image of the patterned AAO template. (b) SEM image of PS nanotube arrays with circular patterns. (c and d) Enlarged SEM images of the PS nanotube arrays.

template after the solvent completely evaporated. PS nanotube arrays were obtained. The schematic diagram of the nanofabrication process is shown in Figure 1.

**2.4. Characterization of PS Nanotubes.** The morphology of the PS nanostructure arrays was investigated using a JEOL JSM-6390LV scanning electron microscope (SEM). The microstructure of the PS nanotubes was investigated using a Philips CM200-FEG transmission electron microscope (TEM). The specimen for TEM observation was prepared by evaporating a drop (5  $\mu\text{L}$ ) of the nanostructure dispersion onto a carbon-film-coated copper grid. XRD analysis was performed on a Bruker D9 Advance with a Cu  $K\alpha$  radiation ( $\lambda = 1.5418 \text{ \AA}$ ).

### 3. Results and Discussion

Figure 2 shows typical SEM images of patterned AAO template and PS nanotube arrays with circular patterns. As shown in Figure 2a, ordered large area circular patterns were obtained in the AAO template. It can be clearly seen that the distance between two adjacent patterns is about 5  $\mu\text{m}$ , and the diameter of each pattern is about 5  $\mu\text{m}$ . The patterns were completely copied from the masks. Figure 1b reveals that the PS nanotube arrays are regular and the naked nanotubes are parallel to each other after the removal of the AAO template. However, Figure 2c shows that the distance between two adjacent clusters is a bit larger than that of the mask, about 6  $\mu\text{m}$ . The reason for this is that a small amount of photoresist

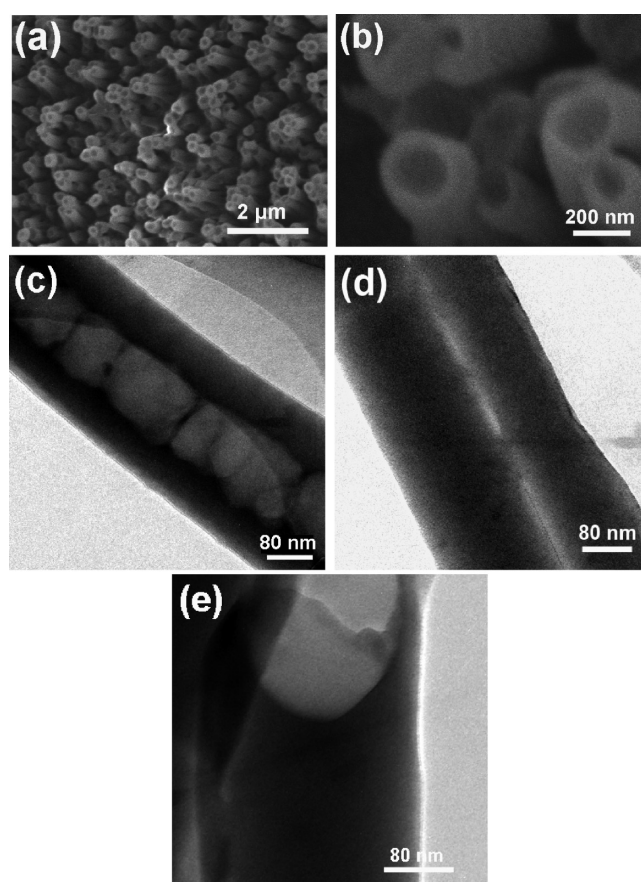
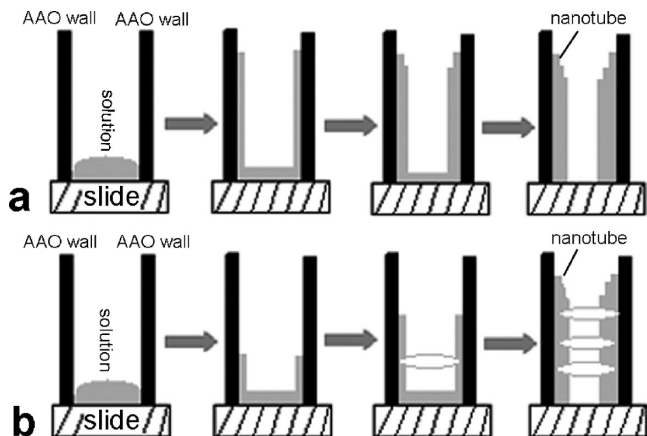


Figure 3. Typical SEM and TEM images of PS nanotubes: (a) a typical SEM image of PS nanotubes; (b) enlarged nanotubes; (c) TEM image of a single bamboo-like nanotube; (d and e) TEM images of barrel-shaped nanotubes.

which remained at the edge of each circular pattern of AAO template still sealed the open pores, and stopped PS nanotubes from going out of the pores. Thus, the diameter of each PS nanotube cluster is smaller than that of the mask, and the distance is a little larger. From Figure 2d, the characteristics of nanotubes can be seen more clearly. However, the length of the nanotubes in the same cluster is not uniform, and the nanotubes at the edge of the clusters broke or fell off. This may be due to the fact that these nanotubes got touched by tweezers when the AAO template was removed.

Figure 3a shows a top view of the PS nanotubes. In Figure 3b, the enlarged top view of the PS nanotubes shows clearly open ends. Just as shown in Figure 3c–e, the wall thickness of the PS nanotubes is not uniform during the wetting process.



**Figure 4.** Schematic diagram for the mechanism of wetting the AAO template by polymer solution: (a) schematic diagram for cylinder-shaped nanotubes; (b) schematic diagram for bamboo-like nanotubes.

The wall thickness of the PS nanotubes in Figure 3c is thinner than that in Figure 3d but is much thicker than that in Figure 3e (the PS nanotubes in Figure 3c–e came from the same 2.5 wt % solution). The microstructure of the nanotubes is different. It is clearly presented in TEM images that the nanotube in Figure 3c is bamboo-like and the nanotubes in Figure 3d and e are cylinder-shaped. However, the wall thickness of the nanotubes in Figure 3e is much thinner than that in Figure 3d. The reason is that the wetting process in every inner nanopore is different. The nanotube diameter is from 200 to 300 nm.

On the basis of our experimental results, a vivid schematic diagram is given to help us better understand the mechanism of wetting the AAO template by polystyrene solution. Figure 4 illustrates the schematic diagrams of the wetting process for PS nanotubes. An understanding of the wetting mechanism of cylinder-shaped PS nanotubes is clear from Figure 4a. The explanation for the formation of cylinder-shaped PS nanotubes is as follows. Because the inner surfaces of template nanopores have a very high surface energy, when polymeric solution goes through the open nanopores, it will wet the nanoporous wall first and form a wetting layer. The wetting layer extends along the porous wall to cover the whole template surface. The first wetting makes the PS solution rise to a certain height along the walls, and the second wetting makes the PS solution reach the same height or a location lower than the first time wetting, and so on. The wetting process could be carried on repeatedly and will not stop until the solvent completely evaporated.<sup>9</sup> The walls of the nanotubes increase in thickness gradually, but they do not have the same thickness because of the different morphology of the inner walls and possible concentration gradient on the surface liquid drop.

The wetting mechanism of bamboo-like nanotubes, just like that of cylinder-shaped nanotubes, is a multiwetting mechanism (Figure 4b). The difference is that the first wetting makes the solution rise to a lower position along the wall. However, the rest of the wetting is higher than before, and marks were left at every wetted place. Thus, the bamboo-like nanotubes come into being after the solvent completely evaporated.

It is well-known that polystyrene has a low degree of crystallinity and crystalline polystyrene should be formed in spherocrystal. Figure 5 presents a typical HRTEM image of the side wall of the PS nanotube. We can see clearly from this image that crystalline lattice fringes exist in some regions and the lattice spacing is measured to be 3.3 Å, while most regions show an amorphous nature.

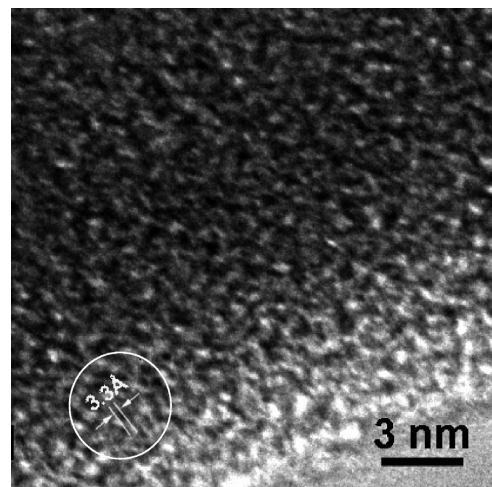


**Figure 5.** HRTEM image of the sidewall of a single PS nanotube.

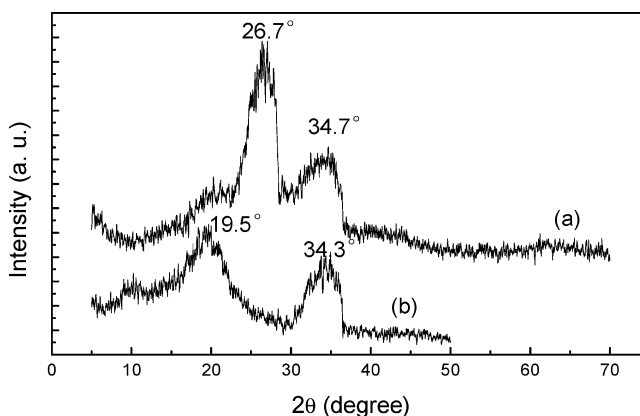


**Figure 6.** XRD spectra of polystyrene: (a) PS nanotubes; (b) bulk PS.

XRD is used to compare the degree of crystallinity for PS nanotubes and the bulk PS. Figure 6 shows the XRD pattern collected from both nanotubes and bulk PS. From Figure 6, it can be seen that there are two major peaks at 19.5 and 34.3° for bulk PS, while there are two peaks at 26.7 and 34.7° for PS nanotubes. According to the Bragg equation,  $2d \sin \theta = n\lambda$ , the corresponding lattice spacings are 3.33 and 2.58 Å for PS nanotubes, which is consistent with our HRTEM observation. It can be seen that the PS nanotubes have a higher degree of crystallinity than the bulk PS because the peak at 26.7° is narrower than the other peaks for the bulk PS.

#### 4. Conclusion

In summary, ordered polystyrene nanotubes have been fabricated by the polymer solution-wetting method in porous alumina templates. HRTEM imaging shows that there are lattice fringes in some regions of the PS nanotubes. XRD analysis indicates that PS nanotubes have a higher degree of crystallinity than bulk PS. According to the PS solution-wetting process, we proposed two types of multiwetting mechanisms for the formation of PS nanotubes. These two growth mechanisms can be applied to other polymer nanostructures and wetting processes using a low concentration of polymer solutions. Various metal nanowires can be deposited into polymer nanotubes in order to fabricate nanocables for nanodevices. Our group has prepared nanocables of Polyamide 6 nanotubes enveloping Pt nanowires.<sup>21</sup> We are trying to assemble microdevices using nanocable arrays with patterns obtained by photolithography.

**Acknowledgment.** This work was supported by the National Natural Science Foundation of China (no. 50473012) and the Natural Science Foundation of Shandong Province (no. Z2005F03).

### References and Notes

- (1) MacDiarmid, A. G. *Angew. Chem., Int. Ed.* **2001**, *40*, 2581.
- (2) Funk, S.; Hokkanen, B.; Burghaus, U.; Ghicov, A.; Schmulki, P. *Nano Lett.* **2007**, *7*, 1091.
- (3) Wang, C. C.; Kei, C. C.; Yu, Y. W.; Perng, T. P. *Nano Lett.* **2007**, *7*, 1566.
- (4) Shimizu, T.; Masuda, M.; Minamikawa, H. *Chem. Rev.* **2005**, *105*, 1401.
- (5) Steinhart, M.; Wehrspohn, R. B.; Gosele, U.; Wendorff, J. H. *Angew. Chem., Int. Ed.* **2004**, *43*, 1334.
- (6) Bong, D. T.; Clark, T. D.; Granja, J. R.; Ghadiri, M. R. *Angew. Chem., Int. Ed.* **2001**, *40*, 988.
- (7) Goldberger, J.; He, R.; Zhang, Y.; Lee, S.; Yan, H.; Choi, H.-J.; Yang, P. *Nature* **2003**, *422*, 599–602.
- (8) Chiou, N. R.; James, L.; Epstein, A. J. *Chem. Mater.* **2007**, *19*, 3589.
- (9) She, X. L.; Song, G. J.; Li, J. J.; Han, P.; Yang, S. J.; Wang, S. L.; Peng, Z. *Polym. J.* **2006**, *38*, 639.
- (10) Li, X. R.; Song, G. J.; Peng, Z.; She, X. L.; Li, J. J.; Sun, J.; Zhou, D.; Li, P. D.; Shao, Z. *J. Nanoscale Res. Lett.* **2008**, *3*, 521.
- (11) Imran; Mousa, M. A. *J. Alloys Compd.* **2008**, *455*, 17.
- (12) Hong, K. Q.; Xie, M. H.; Hu, R.; Wu, H. S. *Appl. Phys. Lett.* **2007**, *90*, 173121.
- (13) Ma, Z.; Liu, Q.; Cui, Z. M.; Bian, S. W.; Song, W. G. *J. Phys. Chem. C* **2008**, *112*, 8875.
- (14) Peng, K.; Huang, Z.; Zhu, J. *Adv. Mater.* **2004**, *16*, 73.
- (15) Wallraff, G. M.; Hinsberg, W. D. *Chem. Rev.* **1999**, *99*, 1801.
- (16) Li, F.; Zhu, M.; Liu, C. G.; Zhou, W. L.; Wiley, J. B. *J. Am. Chem. Soc.* **2006**, *128*, 13342.
- (17) Yamazaki, K.; Namatsu, H. *Microelectron. Eng.* **2004**, *85*, 73.
- (18) Denoual, M.; Griscom, L.; Toshiyoshi, H.; Fujita, H. *Jpn. J. Appl. Phys., Part 1* **2003**, *42*, 4598.
- (19) Schmid, H.; Michel, B. *Macromolecules* **2000**, *33*, 3042.
- (20) Györfvay, E. S.; O'Riordan, A.; Quinn, A. J.; Redmond, G.; Pum, D.; Sleytr, U. B. *Nano Lett.* **2003**, *3*, 315.
- (21) She, X. L.; Song, G. J.; Peng, Z.; Li, J. J.; Lim, C. T.; Tan, E. P. S.; Lv, L.; Zhao, X. S. *Polym. J.* **2007**, *39*, 1.

JP904254S